CSCE Annual Conference

Growing with youth – Croître avec les jeunes

Laval (Greater Montreal)

June 12 - 15, 2019

STRENGTH AND BEHAVIOR OF HSC CONCRETE BEAMS REINFORCED WITH SAND-COATED BASALT FRP BARS

Shehab Mehany[1], Hamdy M. Mohamed[1], and Brahim Benmokrane[1]

[1] Department of Civil Engineering, Université de Sherbrooke, Sherbrooke, Quebec, Canada.

Abstract: This paper presents the behavior of high-strength concrete (HSC) beams reinforced with basalt fiber-reinforced polymer (BFRP) bars under shear. A total of four full-scale HSC beams without stirrups were constructed and tested up to failure. The specimens measured 3,100 mm long, 200 mm wide, and 400 mm deep and were tested under four-point bending. The main parameter of the study was the amount of longitudinal BFRP reinforcement. Three values were considered in this study (1.75%, 1.26%, and 0.83%). The test beams included three beams reinforced with basalt FRP bars, and one beam reinforced with glass FRP (GFRP) bars. The test results are showed in terms of crack patterns, load-deflection behavior, and failure modes. It was observed that the shear strength increased with the increase in the amount of longitudinal BFRP reinforcement.

1. INTRODUCTION

The steel reinforcement resistance to corrosion in concrete structures considered one of the major problems in worldwide. An alternative solution to that of steel reinforcement for reinforcing concrete structures is fiber-reinforced polymer (FRP) bars because of their resistance to corrosion. Furthermore, FRP materials also have high strength-to-weight ratios (El-Sayed et al. 2006; Mohamed and Benmokrane 2016). ACI 440.1R (2015), CAN/CSA S6 (2014), and CAN/CSA S806 (2012) provide design recommendations for using GFRP, CFRP, and AFRP as the main reinforcement in concrete structures. Wu et al. (2012) reviewed the advantages of BFRP and its application in safe and sustainable structures. They reported that BFRP bars are the most recent FRP composite materials developed to enhance the safety and reliability of structural systems. Elgabbas et al. (2015) investigated the physical, mechanical, and durability characteristics of three types of BFRP bars. The test results indicated that the BFRP bars had good mechanical behavior and could be placed in the same category as grade II and grade III GFRP bars according to tensile modulus of elasticity. Nevertheless, the lack of knowledge on BFRP bars has limited its spread and the relevant applications. Moreover, the current FRP material specifications and design codes do not include BFRP as an FRP alternative.

Using HSC is rapidly increasing in bridges, and other structures because of its superior strength and stiffness. One characteristic of HSC that affects the structural response is the propensity of cracks to pass through the aggregates instead of the concrete matrix because of the major similarity between the strength of aggregate and concrete matrix (Gross et al. 2003; Khuntia and Stojadinovic 2001). El-Sayed et al. (2006) investigated the behavior and shear strength of high-strength concrete slender beams reinforced with FRP bars. A six large-scale reinforced concrete beams without transverse reinforcement (stirrups) using high-strength concrete (f'_c = 65 MPa) along with three beams using normal-strength concrete (f'_c = 35 MPa) were tested. The test parameters were the strength of concrete, and the reinforcement ratio and modulus of elasticity of the longitudinal reinforcing bars. CFRP, GFRP bars, and conventional steel bars were used as

longitudinal reinforcement in their investigation. The test results reported that the high-strength concrete beams exhibited slightly lower relative shear strength compared with normal-strength concrete beams.

2. EXPERIMENTAL WORK

2.1 Specimens Details

Four large-scale HSC beams, including one reinforced with GFRP bars, were prepared and tested under monotonic loading conditions. All tested beams were 3,100 mm long, 200 mm wide, and 400 mm deep. A 250 mm overhang length beyond the supports on each side was provided as anchorage length to avoid bond failures prior to shear failures. The shear span was kept constant at 1000 mm for all tested beams. The side clear cover was a 25 mm. While the vertical clear cover was a 50 mm. All beams were reinforced longitudinally on the bottom with 20 mm (#6) BFRP bars or GFRP bars and no transverse reinforcement. All tested beams had the same concrete strength (79.8 MPa), which was provided by a local ready-mix concrete company. The concrete was discharged into the form directly from the ready-mix concrete truck; an electric vibrator was used to consolidate the concrete and to remove air bubbles. The test matrix was arranged to evaluate the influence of reinforcement ratio of BFRP in HSC beams. Table 1 shows the test matrix, and longitudinal reinforcement details of the beam specimens. Each specimen was identified with a tripartite code. The letters (HSC) refer to the type of concrete. The letters B and G identified specimens as being reinforced totally with BFRP or GFRP reinforcement, respectively. The number indicated the longitudinal reinforcement ratio.

Table 1: Test matrix of beam specimens

Beam ID	f_c' (MPa)	Bar Type	Flexural Reinforcement			
			Bars	ρ, %	ρ_b, %	ρ / ρ_b
HSC-B-1.75	79.8	BFRP	4 No.6	1.75	0.325	5.38
HSC-B-1.26	79.8	BFRP	3 No.6	1.26	0.325	3.85
HSC-B-0.83	79.8	BFRP	2 No.6	0.83	0.325	2.55
HSC-G-0.83	79.8	GFRP	2 No.6	0.83	0.454	1.83

2.2 Material Properties

In this study, two types of sand-coated FRP bars were used to reinforce the HSC beams as a longitudinal reinforcement: basalt FRP (BFRP) and glass FRP(GFRP), see Figure 1. Sand coating was used on the surface of the longitudinal bars to enhance the bond between the bars and concrete, as shown in Figure 2. The BFRP, and GFRP reinforcement were manufactured with the same technique by pultruding basalt, and continuous E-glass fibers, respectively, impregnated with a thermosetting vinyl-ester resin. The fiber contents in percentage by weight were 81%, and 83.2% for the BFRP, and GFRP bars, respectively. The tensile properties of BFRP and GFRP bars, the tensile strength and modulus of elasticity, were determined according to ASTM D7205 (ASTM 2011), as reported in Table 2. All of the beam specimens were cast on the same day using normal-weight, ready-mixed concrete with a target compressive strength of 70 MPa after 28 days. The mixture proportion per cubic meter of concrete was as follows: coarse aggregate content of 998 kg with a size ranged between 5 and 10 mm, fine aggregate content of 730 kg, cement content of 510 kg, water-cement ratio (w/c) of 0.32, superplasticizer content of 830 ml/100 kg, and water-reducing agent of 250 ml/100 kg. Based on 100 × 200 mm cylinder testing, the actual compressive strength was 79.8 MPa.

Table 2: Mechanical properties of the BFRP and GFRP bars

Bar Size	d_b (mm)	Area		E_f (GPa)	f_{fu} (MPa)	ε_{fu} (%)
		A_f [a] (mm^2)	A_{im} [b] (mm^2)			
BFRP bars						
#6	20	285	346±2.2	63.7±0.80	1646±40	2.50±0.1
GFRP bars						
#6	20	285	325±1	64.2±0.48	1382±12	2.15±0.1

a Nominal cross-sectional area.
b Immersed cross-sectional area (measured).
Note: Properties calculated based on the nominal cross-sectional area.

(a) Beam cage (b) Cages inside wooden formwork

Figure 1– Beam specimens Details.

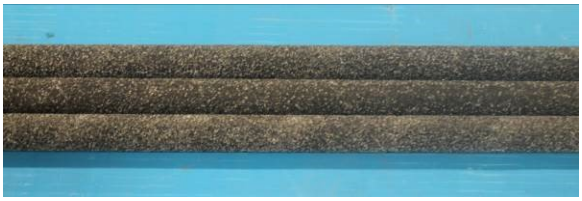

(a) BFGRP bars #6

(b) GFRP bars #6

Figure 2– FRP bar types and surface characteristics.

2.3 Test Setup and Instrumentation

Strains in the longitudinal reinforcing bars were measured using electrical-resistance strain gages with gage lengths of 6 mm bonded on reinforcing bars. The strain gages for reinforcement were located on the center span. In addition, two bonded strain gauges with gage lengths of 60 mm on the concrete at mid-span. One of concrete strain gauges was located at center span on the top surface of the beam. While the other one was located on the beam side at 5 cm from the top surface. Three linear potentiometers (LPOTS) were installed on each beam to measure deflection at different locations during testing. Moreover, one LVDT was installed at the position of the first flexural crack to capture the crack width, See Figure 3. The tests were conducted in the structural lab of the Department of Civil Engineering at the University of Sherbrooke. The beams were tested under four-point bending over a simply supported beam with a clear span and a shear span of 2600 mm and 1000 mm, respectively. The materials testing system (MTS) machine with maximum capacity of 1000 KN was used to apply monotonic load up to failure. The load was applied at a displacement-controlled rate of 0.8 mm/min to avoid any accidental problems associated with the sudden failure, as shown in Figure 4. An automatic data-acquisition system observed by a computer was used to record all data of the test during loading. In addition, crack formation was marked and recorded.

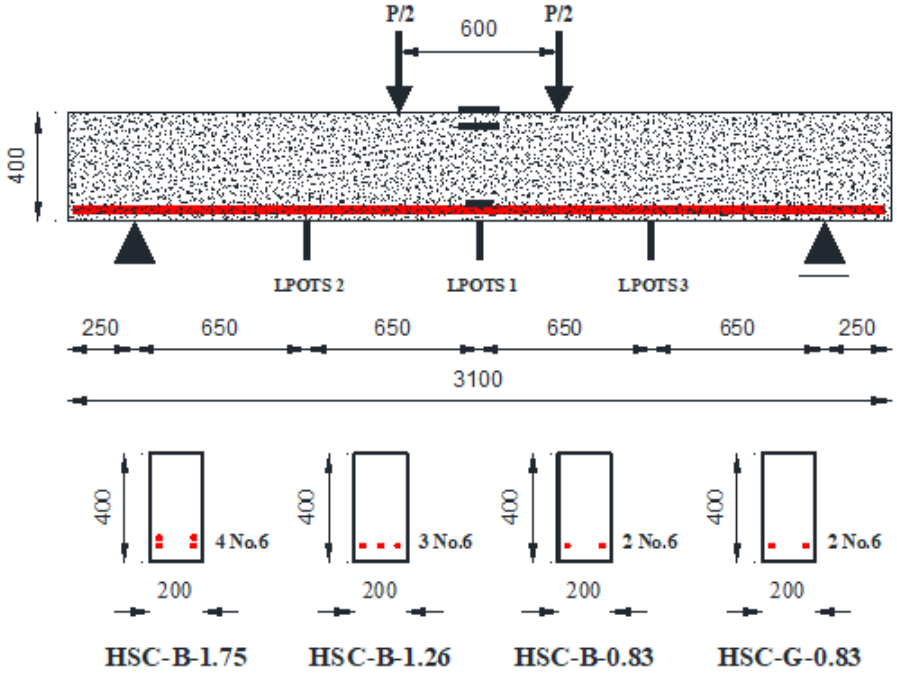

All dimensions in mm

Figure 3– Dimensions, reinforcement details, and strain-gauge locations of the test specimens.

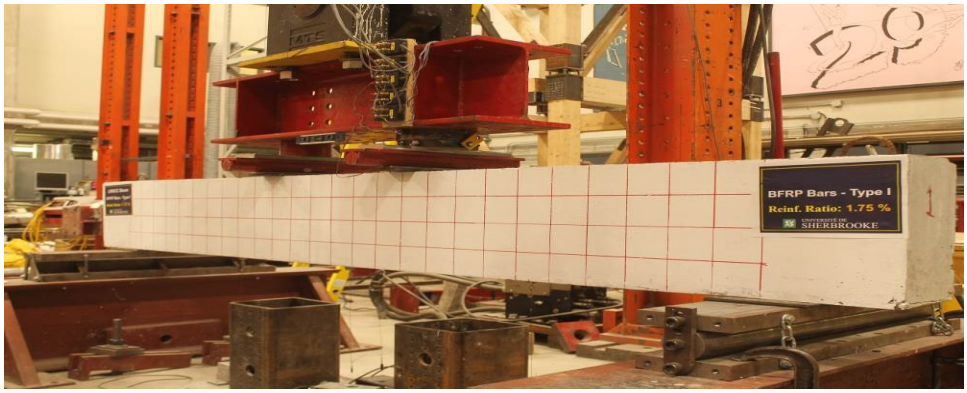

Figure 4– A specimen during testing.

3. EXPERIMENTAL RESULTS

3.1 Crack Patterns and Mode of Failure

The crack patterns and propagation just before the final failure of the tested beams are presented in Figure 5. Cracking was initiated in the flexural span between the two concentrated loads where the flexural tension stress is highest and shear stress is zero. During loading, several flexural cracks were developed in the constant moment region. As the load was increased, one of the flexural cracks extended into inclined crack and developed close to the edge of the support, or an inclined crack formed and observed at the midheight of the shear span. Because of the presence of shear stresses, the inclined shear cracks became progressively more inclined and propagated towards the load point.

Based on Figure 5(b), specimen HSC-B-0.83, a secondary bond-anchorage failure occurred within the shear span at the interface between the concrete and longitudinal reinforcement. This was typically observed to occur concomitantly with the shear collapse. Due to the smoother surface of the shear crack of HSC beams, the contribution of aggregate interlock in transferring shear stresses transfer across the section became less significant, resulting in sudden increase in dowel action to maintain cross sectional equilibrium. These dowel forces cause higher vertical tensile stresses in the concrete surrounding the bars. This secondary splitting failure has been reported in experimental shear tests (Gross et al., 2003). As it can be expected, It was observed that all beams failed in a brittle manner, as a sudden load drop occurred, upon which the beams reached the ultimate shear capacity. The tested beams with higher ρ/ρ_b ratios had slightly more formed cracks prior to failure.

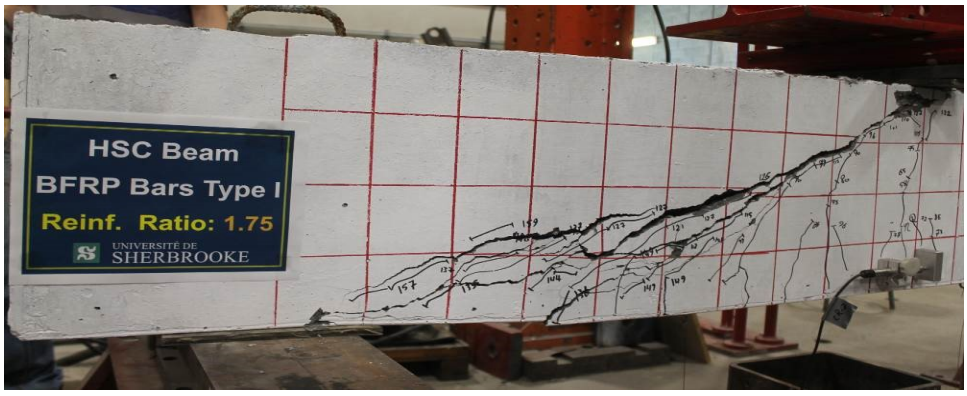

(a) HSC-B-1.75

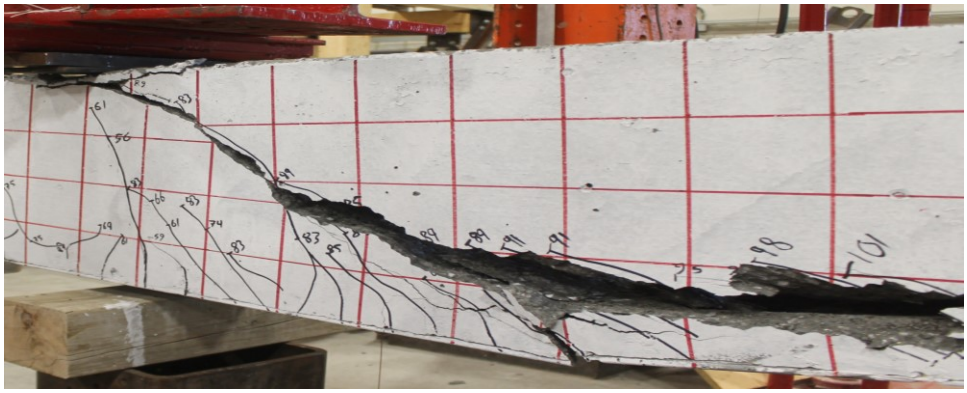

(b) HSC-B-0.83

Figure 5– Final crack pattern.

3.2 Load-deflection response

The influence of the different reinforcement ratios on the load-deflection response of the four beams is shown in Figure 6. It can be observed that the relationship of load-deflection was bilinear. The first stage of the load-deflection curve for all beams exhibited a linear response until reaching flexural cracking. The second stage, after cracking, all specimens showed a significant loss of stiffness with a considerable increase in their point loads deflections. The decreased stiffness varied because of the different reinforcement ratios. It can be noticed that increasing the reinforcement ratio resulted in higher stiffness and decreased its deflection at all stages of loading. Specimen HSC-B-1.75 had a deflection of 19 mm compared with 21.64 mm for beam HSC-B-1.26. Moreover, increasing the reinforcement ratio from 1.26 to 1.75 % resulted an increase in its stiffness at all stages of loading as can be depicted from Figure 6. The results indicated that the load deflection relationships of beams HSC-B-0.83 and HSC-G-0.83 with the same axial stiffness ρE_f were similar. It can be noticed that HSC-G-0.83 showed a slightly higher post-cracking stiffness and higher ultimate capacity than HSC-B-0.83.

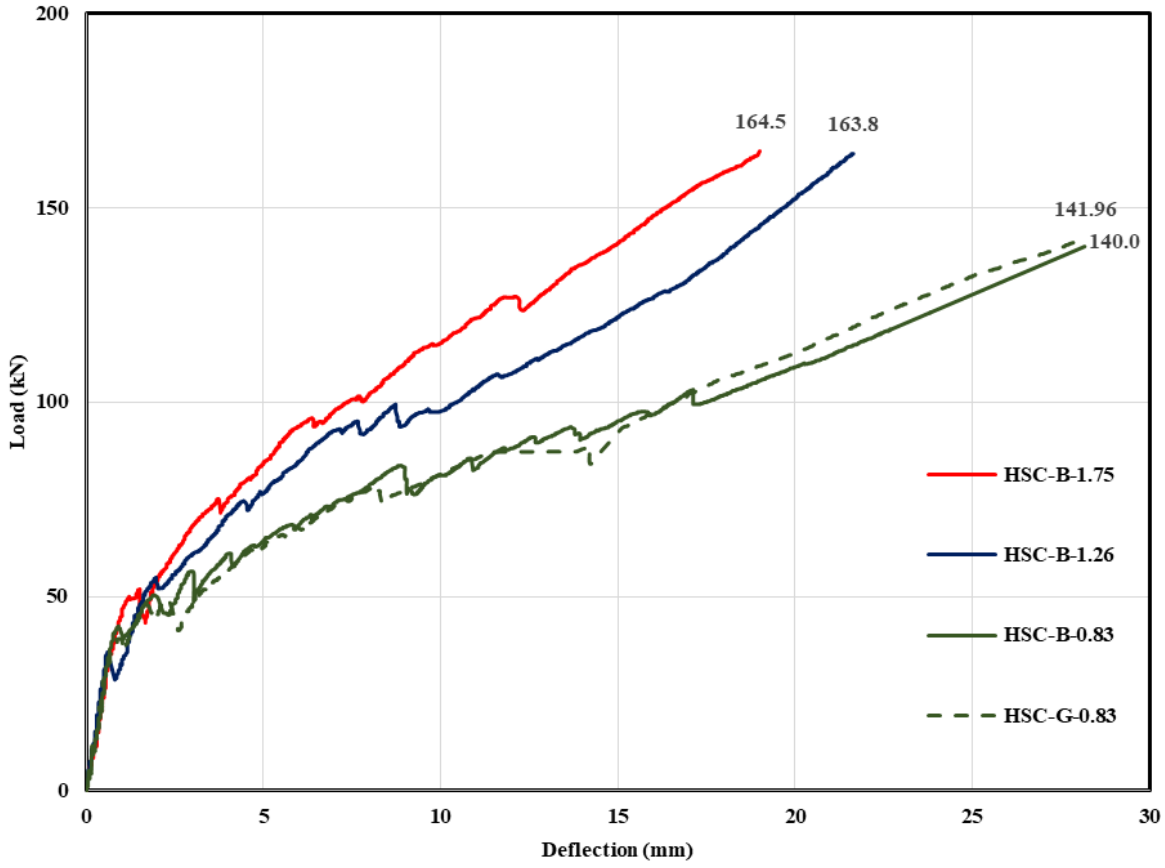

Figure 6– Load-deflection response of beams with different reinforcement ratio.

3.3 Reinforcement and concrete strains

The maximum concrete compressive strains at failure ranged between 1,141 and 1,788 microstrain, which are less than the ultimate crushing strain of 3,500 microstrain by the CSA standards and 3000 microstrain by the ACI code. It is clear that no flexural compression failure had occurred. Furthermore, no signs of flexural compression failure were noticed during testing. The maximum measured tensile strains in FRP bars at failure ranged from 4,416 to 7,025 microstrain, which did not reach 50% of the bars' ultimate tensile strain during the tests.

3.4 Effect of the BFRP longitudinal reinforcement ratio

Figure 7 shows the influence of reinforcement ratio of the BFRP bars on the shear strength of the HSC beams. The vertical axis represents the experimental load of the tested beams. While, the horizontal axis represents the reinforcement ratio ρ. it was found that the shear strength increased as the reinforcement ratio was increased. The shear strength increased by 17.25 % when the longitudinal reinforcement ratio increased by 51.8% (from 0.83 to 1.26%) for the beams reinforced with BFRP. While, increasing the reinforcement ratio by 38.9% (from 1.26 to1.75%) exhibited slightly lower relative shear strength.

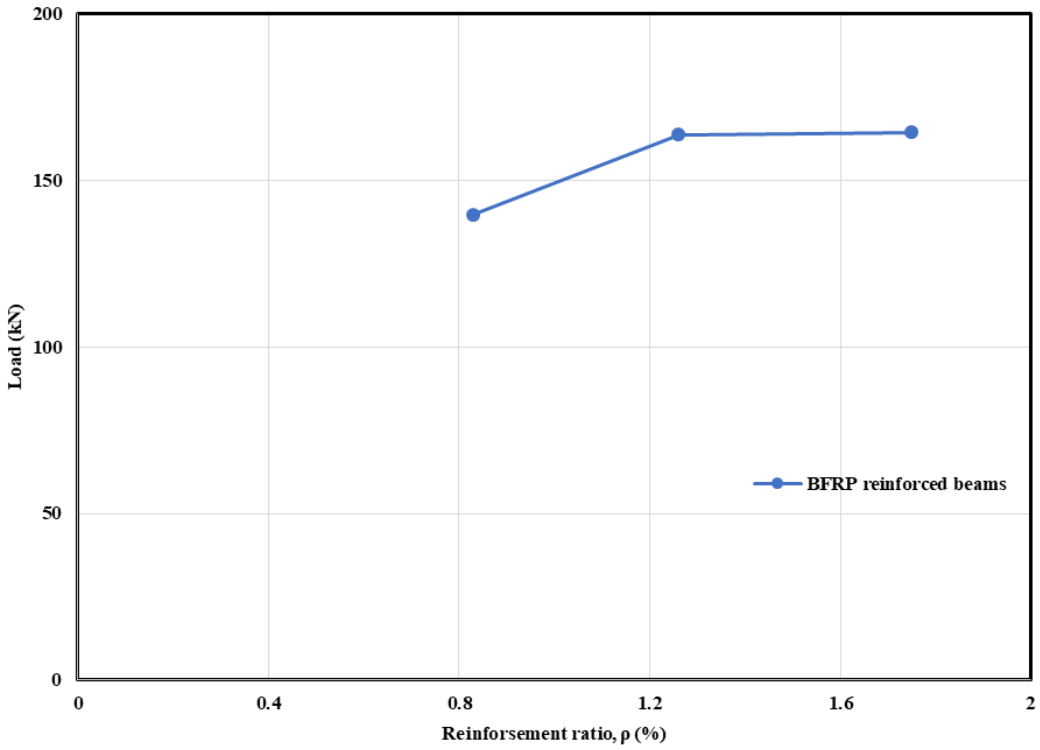

Figure 7– Experimental load versus reinforcement ratio for BFRP reinforced beams.

4. CONCLUSIONS

The test results concerning the shear behavior of full-scale beams reinforced with BFRP bars without stirrups are presented and discussed. The main parameter was the BFRP longitudinal reinforcement ratio. A total of four FRP RC beams of 3,100 mm long, 200 mm wide, and 400 mm deep were cast and tested under four-point bending. The main conclusions and observations of this study can be summarized as follows:

- The test results indicated that the HSC beams reinforced with BFRP bars exhibited similar cracking behavior to those of beams using GFRP bars.

- Based on the experimental results, the shear strength of HSC beams reinforced with BFRP increased with increasing the longitudinal reinforcement ratio. Increasing the BFRP reinforcement ratio from 0.83 to 1.26 % increased the shear capacity of the tested beams by 17.25%. Furthermore, Increasing the BFRP longitudinal reinforcement ratio resulted in higher stiffness and decreased deflections at all loading stages.

ACKNOWLEDGMENTS

The authors would like to acknowledge and gratitude the financial support from the Natural Science and Engineering Research Council of Canada (NSERC), Pultral Inc. (Thetford Mines, Quebec), the technical staff of the structural lab of the Department of Civil Engineering at the University of Sherbrooke.

REFERENCES

ACI Committee 440 (2015). “Guide for the Design and Construction of Concrete Reinforced with FRP Bars (ACI 440.1R-15).” ACI, Farmington Hills, Michigan, USA.

Benmokrane, B., El-Salakawy, E., El-Ragaby, A., and Lackey, T. (2006). “Designing and testing of concrete bridge decks reinforced with glass FRP bars.” J. Bridge Eng., 10.1061/ (ASCE) 1084-0702(2006)11: 2(217): 217–229.

Canadian Standards Association (2012). “Design and Construction of Building Structures with Fiber Reinforced Polymers (CAN/CSA S806-12).” Rexdale, ON, Canada.

Canadian Standards Association (2014). “Canadian Highway Bridge Design Code (CAN/CSA S6–14).” Rexdale, ON, Canada.

Elgabbas, F., Ahmed, E. A., and Benmokrane, B. (2015). Physical and mechanical characteristics of new basalt-FRP bars for reinforcing concrete structures. Construction and building materials, 95, 623-635.

El-Sayed, A. K., El-Salakawy, E. F., and Benmokrane, B. (2006). Shear strength of FRP-reinforced concrete beams without transverse reinforcement. ACI Structural Journal, 103(2), 235.

El-Sayed, A. K., El-Salakawy, E. F., and Benmokrane, B. (2006). Shear capacity of high-strength concrete beams reinforced with FRP bars. ACI Structural Journal, 103(3), 383.

Gross, S. P., Yost, J. R., Dinehart, D. W., Svensen, E., and Liu, N. (2003). Shear strength of normal and high strength concrete beams reinforced with GFRP bars. In High performance materials in bridges (pp. 426-437).

Khuntia, M., and Stojadinovic, B. (2001). Shear strength of reinforced concrete beams without transverse reinforcement. Structural Journal, 98(5), 648-656.

Mohamed, H., and Benmokrane, B. (2016). Reinforced Concrete Beams with and without FRP Web Reinforcement under Pure Torsion. J. Bridge Eng., 10.1061:1943-5592.

Wu, Z., Wang, X., and Wu, G. (2012). “Advancement of Structural Safety and Sustainability with Basalt Fiber Reinforced Polymers.” Proceedings of 6th International Conference on FRP Composites in Civil Engineering (CICE), Rome, Italy, 29 pp.